JOURNAL OF VIROLOGY, Oct. 1997, p. 7744–7749 Vol. 71, No. 10
0022-538X/97/$04.00+0

Coronavirus Genomic and Subgenomic Minus-Strand RNAs Copartition in Membrane-Protected Replication Complexes

PHIROZE B. SETHNA† AND DAVID A. BRIAN*

Department of Microbiology, University of Tennessee, Knoxville, Tennessee 37996-0845

Received 14 April 1997/Accepted 17 June 1997

The majority of porcine transmissible gastroenteritis coronavirus plus-strand RNAs (genome and subgenomic mRNAs), at the time of peak RNA synthesis (5 h postinfection), were not found in membrane-protected complexes in lysates of cells prepared by Dounce homogenization but were found to be susceptible to micrococcal nuclease (85%) or to sediment to a pellet in a cesium chloride gradient (61%). They therefore are probably free molecules in solution or components of easily dissociable complexes. By contrast, the majority of minus-strand RNAs (genome length and subgenomic mRNA length) were found to be resistant to micrococcal nuclease (69%) or to remain suspended in association with membrane-protected complexes following isopycnic sedimentation in a cesium chloride gradient (85%). Furthermore, 35% of the suspended minus strands were in a dense complex (1.20 to 1.24 g/ml) that contained an RNA plus-to-minus-strand molar ratio of approximately 8:1 and viral structural proteins S, M, and N, and 65% were in a light complex (1.15 to 1.17 g/ml) that contained nearly equimolar amounts of plus- and minus-strand RNAs and only trace amounts of proteins M and N. In no instance during fractionation were genome-length minus strands found segregated from sub-genome-length minus strands. These results indicate that all minus-strand species are components of similarly structured membrane-associated replication complexes and support the concept that all are active in the synthesis of plus-strand RNAs.

Coronaviruses are single-stranded, plus-strand RNA viruses with a genome of approximately 30 kb (19). During replication in the cytoplasm, they produce not only a minus-strand copy of the genome (i.e., the antigenome) but also minus-strand copies of the six to eight 3′-coterminal subgenomic mRNAs (15, 16, 32, 33). The abundance of the subgenomic minus-strand species (0.1 to 0.01 the level of mRNAs) (16, 33), the kinetics of subgenomic minus-strand RNA synthesis relative to subgenomic mRNA synthesis (16, 33), the presence of synthetically active double-strand subgenomic replicative (or transcriptive) forms (29), and the analysis of mutant viruses temperature sensitive for minus-strand synthesis (31) have all indicated that the subgenomic minus-strand RNAs are active in the synthesis (i.e., amplification) of mRNAs. Initially (33) it was envisioned that the subgenomic mRNAs, generated perhaps by a leader-priming mechanism (19), were the templates for subgenomic minus-strand RNA synthesis. In this scheme, minus strands thus generated would be templates for mRNA amplification by a replication model (16, 33). More recent experimentation (9, 29, 30) has suggested that the subgenomic minus-strand RNAs with fused 3′-terminal antileaders (32) may be the first molecules generated and that they then serve as templates for subgenomic plus-strand synthesis (30). The in vivo synthesis of plus strands from T7 RNA polymerase-transcribed minus strands in virus-infected cells (14) would seem to support this second model. Neither of the models, however, has been proven by direct experimentation in an in vitro system, nor has it been directly determined in vitro whether intergenic promoters within subgenomic minus-strand RNAs can serve as templates for the synthesis of mRNAs of smaller size (7).

In an effort to develop an in vitro system to examine these issues, we began with the membranous postnuclear fraction of porcine transmissible gastroenteritis coronavirus (TGEV)-infected cells known to contain RNA-dependent RNA polymerase activity (11). During attempts to remove endogenous viral RNA templates, we learned that viral plus-strand RNAs (approximately 15% of the total) and minus-strand RNAs (approximately 69% of the total) were protected from micrococcal nuclease digestion in membranous complexes. The membranous complexes containing the majority of minus-strand RNA species, furthermore, could be resolved by isopycnic sedimentation in a CsCl gradient into two general populations. The denser population (1.20 to 1.24 g/ml) contained plus-to-minus-strand molar ratios averaging 8:1 among all RNA species along with the S, M, and N virus structural proteins, whereas the lighter population (1.15 to 1.17 g/ml) contained plus-to-minus-strand molar ratios averaging nearly 1:1 and only very minor amounts of the M and N proteins. In all fractions, regardless of the procedure used for preparation, genome-length and subgenome-length minus strands were found together in amounts reflecting relative mRNA abundancies in whole-cell preparations. This distribution supports the view that antigenome and subgenomic minus-strand RNAs function similarly in plus-strand RNA synthesis. We postulate, furthermore, that the denser population represents complexes used primarily for abundant synthesis of mRNAs that become immediately available for translation.

MATERIALS AND METHODS

Cells and virus. Plaque purification of the Purdue strain of TGEV from an infectious genome and preparation of virus stocks between passages 3 and 10 on swine testicle cells have been described previously (6, 17).

Preparation and experimental treatment of the RNA-dependent RNA polymerase-containing postnuclear fraction. Infection of cells, cell lysis, and preparation of the postnuclear fraction were done as previously described (11) except that the ionic detergent deoxycholate (0.28% [wt/wt], final concentration) was omitted in the last step unless otherwise indicated. Briefly, 4×10^7 cells (2-150-cm^2 flasks) were infected with a multiplicity of 10 PFU/cell; at 5 h postinfection, cells were washed five times with ice-cold TN buffer (10.0 mM Tris [pH 7.4], 100 mM NaCl) and harvested by scraping and pelleting. Cells were gently resuspended in 1 ml of 0.3 M sucrose made up in RNase-free water, held on ice

* Corresponding author. Phone: (423) 974-4030. Fax: (423) 974-4007. E-mail: dbrian@utk.edu.

† Present address: Glaxo Wellcome Inc., Research Triangle Park, NC 27709.

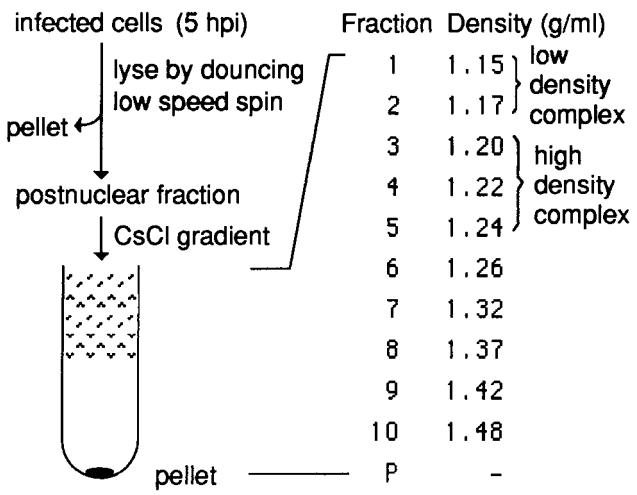

FIG. 1. Scheme for the preparation of the postnuclear fraction and its fractionation on a CsCl gradient. The buoyant densities of the fractions, recovered from the top, are shown. hpi, hours postinfection.

for 10 min, and then broken by 15 strokes in a tight-fitting 5-ml Dounce homogenizer. Nuclei were pelleted at 650 × *g* for 7 min; the supernatant (approximately 1 ml) was adjusted to contain 50 mM Tris-HCl (pH 8.0) and 40 μg of dextran sulfate per ml and called the postnuclear fraction. For sedimentation analysis, the postnuclear fraction (0.6 ml/gradient) was either (i) loaded directly onto a cesium chloride gradient (Fig. 1), (ii) treated with micrococcal nuclease before loading, or (iii) treated with detergent before loading.

For micrococcal nuclease treatment, essentially the method of Miller and Hall (21) was used except that detergent was omitted from the digestion mix unless otherwise indicated. Briefly, the postnuclear fraction was made 625 μM $CaCl_2$ and then incubated with 0.6 U of micrococcal nuclease (Boehringer Mannheim) per ml at room temperature for 30 min. The reaction was stopped by the addition of 0.1 volume of 0.5 M EGTA (pH 8.0). For treatment with detergent, the postnuclear fraction was made either 0.28% (wt/wt) deoxycholate (11) or 0.1, 0.25, or 1.0% (vol/vol) Nonidet P-40 and incubated for 30 min at room temperature before nuclease treatment.

Isopycnic sedimentation in a cesium chloride gradient. The method of Raju et al. (27) was used. Briefly, 0.6 ml of the indicated preparation was layered onto a 4.4-ml linear gradient of 20 to 40% (wt/wt) CsCl made up in TNE buffer (10 mM Tris-HCl [pH 7.4], 150 mM NaCl, 1 mM EDTA), and the gradient was centrifuged at 45,000 rpm in an AH650 rotor (Sorvall) for 16 h at 10°C. Fractions of 0.5 ml were collected by micropipetting from the top and used directly for RNA extraction or protein analysis or were first dialyzed for 2.5 h against TNE at 4°C in a membrane microdialysis apparatus (8-kDa-molecular-mass cutoff) (Bethesda Research Laboratories) before further treatment. Buoyant densities were determined from the refractive indices.

RNA blot (Northern) analysis. Northern analyses were done as previously described (33). Briefly, extracted RNA was denatured with formaldehyde-formamide, electrophoresed on a 1% agarose gel in the presence of formaldehyde, vacuum blotted onto a positively charged nylon membrane, and probed. Probe 1 (5′-CAGCATGGAGAAGACGAGCATCTCG-3′), which binds within the HP gene (17, 37), and probe 2 (the complement of probe 1) were 5′ end labeled with [γ-^{32}P]ATP (ICN Biochemicals, Irvine, Calif.) and polynucleotide kinase and used to detect plus and minus strands, respectively. Specific activities, which ranged from 1.5 to 3.5 × 10^6 cpm/pmol, differed between the two probes by no more than 18% for any preparation and was a difference accounted for when molar ratios were determined. Blots were analyzed quantitatively with the Bio-Rad GS-670 Densitometer, Molecular Analyst system.

Protein blot (Western) analysis. One-half of each 500-μl fraction from the CsCl gradient was used for protein analysis. Proteins were precipitated with 3 volumes of acetone at −20°C, recovered by sedimentation at 14,000 × *g* for 10 min, dissolved in 15 μl of 50 mM Tris-HCl (pH 8.0), and subjected to sodium dodecyl sulfate-polyacrylamide gel electrophoresis on a gel of 12% polyacrylamide. Proteins were transferred to nitrocellulose by electrophoresis, and virus-specific proteins were identified by Western blotting using a 1:10 dilution of TGEV-specific hyperimmune porcine serum (a gift from L. Kemeny, National Animal Disease Laboratory, Ames, Iowa) and ^{125}I-protein A (ICN) as described previously (18, 37).

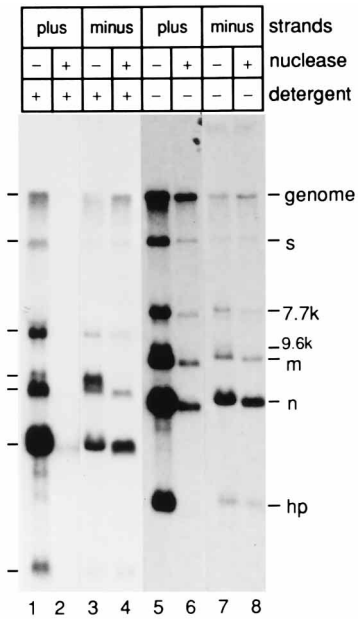

FIG. 2. Resistance of viral RNA species in the postnuclear fraction to micrococcal nuclease. RNA was extracted from the postnuclear fraction after the specified treatment and analyzed by Northern analysis. Blots were probed with end-labeled oligodeoxynucleotides that specifically detect plus- or minus-strand RNAs (33). Lanes 1 to 4, the postnuclear fraction was resuspended in 0.28% deoxycholate as described in reference 11 prior to micrococcal nuclease treatment; lanes 5 to 8, the postnuclear fraction was resuspended in the absence of detergent prior to micrococcal nuclease treatment. mRNA species (identified) are named for the proteins encoded by their 5′-proximal open reading frames (33). Minus-strand RNA species (not identified) migrate to positions near those of their plus-strand counterparts.

RESULTS

The majority of coronavirus intracellular minus-strand RNAs are found in membrane-protected complexes. In attempts to develop an in vitro coronavirus RNA-synthesizing system responsive to exogenously added RNAs, the postnuclear fraction of TGEV-infected cells containing 0.28% (wt/wt) deoxycholate (11) was treated with micrococcal nuclease to remove endogenous RNA templates. Micrococcal nuclease, which digests both single- and double-stranded RNA and DNA to mononucleosides in a reaction controlled by the concentration of Ca^{2+}, has been successfully used in the presence of nonionic detergent to render brome mosaic virus preparations free of endogenous templates and responsive to exogenously added RNA (21). Although we have so far been unable to show responses to added synthetic mRNA templates, or to their complementary minus strands, from these experiments we observed surprisingly that whereas 83% of the intracytoplasmic plus-strand RNA species (genome and subgenomic mRNAs) were eliminated by treatment with micrococcal nuclease, only 18% of minus strands were similarly removed (Fig. 2, lanes 1 to 4). In the absence of the deoxycholate, these percentages became 85 and 31%, respectively (averages of three experiments) (Fig. 2, lanes 5 to 8), indicating that deoxycholate at this concentration had little effect on the protection of viral RNA species. Our surprise stemmed from a presumption that membranes would have been sufficiently disrupted by the detergent to render all RNAs susceptible to nuclease. These results prompted an investigation into how minus strands are compartmentalized relative to one another and to plus strands.

The resistance of the minus-strand RNAs to micrococcal

nuclease in the presence of detergent suggested that they were perhaps protected as tightly configured ribonucleoprotein (RNP) complexes as found for the genomic and antigenomic RNAs of the nonsegmented and some segmented negative-strand animal viruses (23, 27) (the segmented influenza virus RNPs are susceptible to RNase digestion [26]) or were protected, despite the presence of 0.28% deoxycholate, by lipid membranes possibly similar to those associated with replication complexes of the plus-strand picornaviruses (4) and alphaviruses (2, 13). To distinguish between these possibilities, the postnuclear fraction was subjected to isopycnic sedimentation in a CsCl gradient of 1.19 M (1.17 g/ml) to 2.28 M (1.42 g/ml) (Fig. 1), either with or without prior treatment with 0.1, 0.25, or 1.0% (vol/vol) Nonidet P-40, a detergent that at a concentration of 1% is known to release coronavirus RNPs (35). A stable RNP complex would be expected to band in the gradient with a buoyant density of nearly 1.31 g/ml and to be unaffected by the addition of detergent (27). Membrane-protected complexes in the absence of detergent would also be expected to band in the CsCl gradient, based on experiments with membrane-limited organelles (28), but in the presence of detergent would be expected to disassemble. RNA released from the complex would be expected to pellet. As illustrated in Fig. 3A, lanes 1 to 11, and 3B, lanes 1 to 11, when the postnuclear fraction was prepared with no detergent and sedimented, 39% of plus strands and 85% of minus strands (averages of three experiments) were found banded in the top five fractions of the gradient between buoyant densities of 1.15 and 1.24 g/ml, the only region of the gradient showing cloudy bands. The remainder of the RNA, which was 61% of plus strands and 15% of minus strands, was found in the pellet. In the presence of 0.25 and 1.0% Nonidet P-40, all of both strands was found in the pellet (data not shown). In the presence of 0.1% Nonidet P-40, a small amount of both plus and minus strands remained suspended in the top five fractions (data not shown). These results indicate that minus strands in the postnuclear fraction are banding not as stable RNPs but as components of membranous complexes requiring, in the case of Nonidet P-40, a detergent concentration of >0.1% for total disruption. Some of the plus-strand species may have been in the membranous complexes as well or possibly in virions at various stages of assembly within pre-Golgi-derived enveloped microsomal structures (36).

It was also ruled out that minus-strand RNAs were protected from micrococcal nuclease by RNP-like structures through experiments in which protease treatment of the postnuclear fraction prepared in the absence of detergent (22) failed to expose the minus-strand RNAs to nuclease (data not shown). Treatments included proteinase K, chymotrypsin, or trypsin at 400 μg/ml (final concentration) for 30 min at 20°C.

To determine whether the plus-strand RNPs from mature virions would be stable enough to remain suspended in a CsCl gradient and thus explain the presence of some of the plus strands in the upper part of the gradient, purified TGEV was treated for 30 min at 20°C with 1% Nonidet P-40 (35) and sedimented. Nearly all of the RNA from Nonidet P-40-treated virions pelleted, but some remained suspended throughout the bottom five fractions (data not shown), establishing that the TGEV genomic RNP is mostly unstable in the CsCl gradient and making it unlikely that the plus-strand RNAs in the upper half of the gradient came from intracellular viral RNPs.

Two types of membranous complexes were found: a denser one containing most of the suspended plus-strand RNAs and a lighter one containing most of the suspended minus-strand RNAs. Although essentially all of the RNA species remaining in suspension after isopycnic sedimentation of the postnuclear fraction were in the top five fractions, the patterns of plus- and minus-strand distribution were not superimposable. Both genomic and subgenomic plus strands were skewed toward the gradient center (i.e., showing greatest abundance in fraction 4 [Fig. 3A, lanes 1 to 5]), whereas the minus strands were skewed toward the top (i.e., showing greatest abundance in fractions 1 and 2 [Fig. 3B, lanes 1 to 5]). On a molar basis, calculated from absorbance in the autoradiograms and specific activities of the probes, plus strands were on average eightfold more abundant than minus strands in fractions 3 through 5 (ranging from nearly 20:1 for genome to 4:1 for N mRNA) but were nearly equal in fractions 1 and 2. The distinctly different skewing patterns of plus and minus strands were found in each of three separate experiments.

To explain the skewing of the plus-strand RNAs toward the gradient center, we postulated that they were in some way associated in high concentration with structures producing mRNAs for immediate translation. We viewed it as unlikely

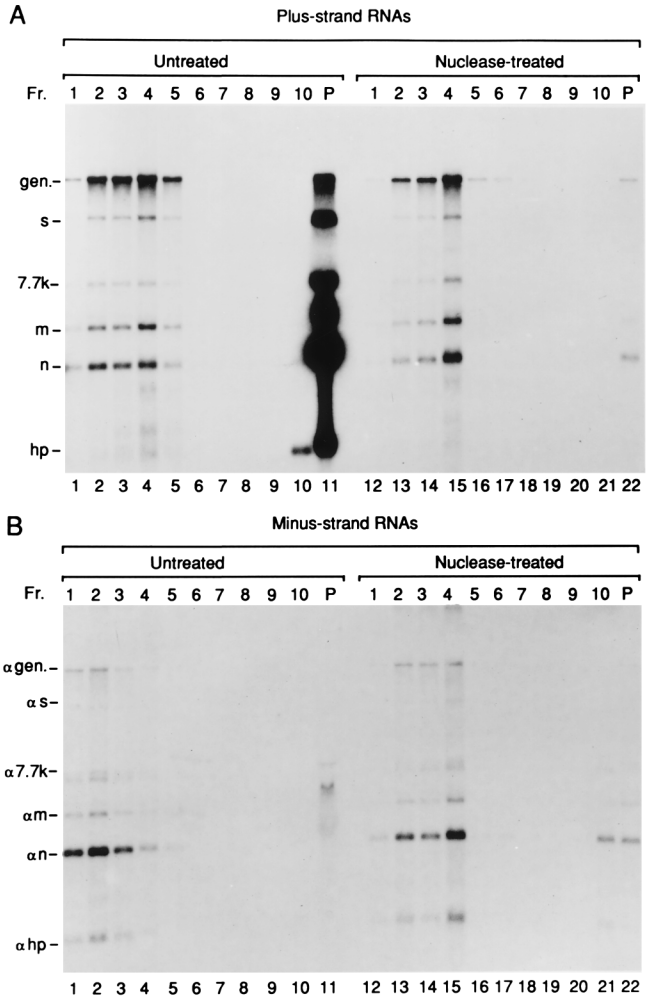

FIG. 3. Distribution of viral RNA species in membrane fractions (Fr.) recovered from a CsCl gradient. (A) Northern detection of plus-strand RNAs. Cytoplasmic lysate was either sedimented directly (lanes 1 to 11) or treated with micrococcal nuclease before sedimentation (lanes 12 to 22). RNA was electrophoresed, blotted, and probed for the detection of plus strands. mRNA species are identified. (B) Northern detection of minus-strand RNAs. Treatments were the same as for in panel A except that RNA was probed for the detection of minus strands. Minus-strand RNA species (indicated by the prefix "α") are identified. gen., genome.

that they, except for possibly some genomic RNA, represented packaged species since TGEV virions contain only minor amounts of subgenomic plus strands (33). We also thought it unlikely that the abundant mRNAs represented components of polyribosomes since the conditions of the gradient, namely, high salt (CsCl) and the presence of a chelating agent (EDTA), are incompatible with polysomal integrity (25). To test whether mRNAs associated with structures in the gradient center are potentially accessible for translation, the postnuclear fraction prepared in the absence of detergent was treated with micrococcal nuclease before sedimentation, and the amounts and distributions of plus and minus strands following nuclease treatment were determined. As illustrated in Fig. 3A, lanes 12 to 16, the plus strands in fractions 1 through 5 were reduced in amount, most notably in fractions 2 and 5, compared to undigested material (Fig. 3A, lanes 1 to 5), suggesting that some of the plus strands are on the surface of membranous structures and therefore probably accessible for translation.

Interestingly, following micrococcal nuclease treatment, the abundance of minus strands in fractions 1 and 2 (Fig. 3B, lanes 1 and 2) was also decreased, but for these there was a corresponding increase in abundance in the gradient center (i.e., primarily in fraction 4 [Fig. 3B, lanes 12 to 15]). Thus, after nuclease treatment, the distributions of plus and minus strands became nearly superimposable and roughly equimolar among the subgenomic species.

To exclude the effects of altered membrane sedimentation properties that might have resulted from the RNase treatment, cytoplasmic lysate was sedimented, fractionated, and dialyzed before the nuclease digestion step and subsequent Northern analysis (Fig. 4). This analysis demonstrated first that there was a net decrease in the amount of plus strands in the gradient center and of minus strands in the gradient top as a result of nuclease digestion, supporting the conclusion that there are surface-adherent molecules of both plus and minus strands on membranous structures in these fractions. Second, the distributions of plus- and minus-strand RNA species remaining after nuclease treatment (appearing most abundantly in fractions 1 and 2 for minus strands and fractions 2 and 3 for plus strands) were essentially equimolar in fractions 1 and 2, suggesting that the RNA-containing membranous complexes with buoyant densities of 1.15 to 1.17 and 1.20 to 1.24 are of fundamentally different composition. Furthermore, the experiment shows that the membranous complexes had undergone changes in sedimentation properties as a result of RNase treatment.

Few if any viral structural proteins are associated with the lighter membrane complex. To determine which virus-specific proteins might be associated with the two membranous populations, proteins collected from one half of each fraction of the gradients illustrated in Fig. 3 were separated by sodium dodecyl sulfate-polyacrylamide gel electrophoresis and analyzed by immunoblotting with porcine hyperimmune anti-TGEV serum (Fig. 5). The serum was preadsorbed with uninfected swine testicle cells and does not detect cellular proteins in the immunoblot but does recognize all three major structural proteins of TGEV (21a). From immunoblots of preparations made in the absence of nuclease (Fig. 5A), it was observed that whereas abundant amounts of proteins the sizes of S, M, and N were found in the region of the high-density complex (fractions 3 through 5), only small amounts of proteins the sizes of M and N were found in the lighter membrane complexes (fractions 1 and 2). This finding suggests, especially from the profile in fraction 1, that there are few viral structural proteins associated with the minus-strand-containing membranous structures. Curiously, fraction 5 of the nuclease-treated fractions had relatively large amounts of protein the sizes of S and N, but not of M, and a greatly diminished RNA content (Fig. 5B), suggesting that the structural proteins in these fractions were probably contributed not by virus particles but by proteins at membrane-associated sites of virus assembly.

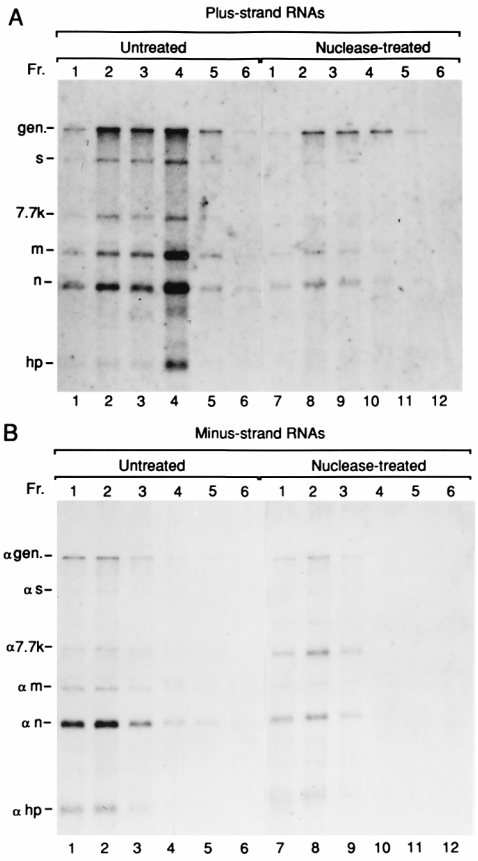

FIG. 4. Distribution of viral RNA species in the top six fractions of a CsCl gradient treated with micrococcal nuclease following sedimentation. The postnuclear fraction (Fr.) prepared in the absence of detergent was isopycnically sedimented in a CsCl gradient, and the fractions were separately dialyzed to remove CsCl. (A) Northern detection of plus-strand RNAs. RNA was extracted directly from the dialyzed fractions (lanes 1 to 6), or the dialyzed fractions were treated with micrococcal nuclease before RNA extraction (lanes 7 to 12), and the RNA was electrophoresed, blotted, and probed for the detection of plus strands. (B) Northern detection of minus-strand RNAs. Treatments were the same as for panel A except that the blot was probed for the detection of minus strands (indicated by the prefix "α"). gen., genome.

DISCUSSION

A common if not universal property among cytoplasmically replicating positive-strand RNA viruses of plants and animals is an intimate association of the RNA-synthesizing machinery with cellular membranes (references 1, 2, 4, 5, 11, 13, 20, 21, 38, and 39 and references therein). In studies in which in vitro viral RNA synthesis was carried out in the presence of nonionic detergents, and thus presumably in the absence of intact membranes, only minus-strand products were found (38, 39). Complete replication in vitro leading to the synthesis of new plus strands from input plus-strand templates has required the presence of membranes (1) or the components of membrane-forming structures (38). Membrane integrity, therefore, appears to be critical for RNA replication, although the mechanistic basis for this requirement is not understood, nor is the precise anat-

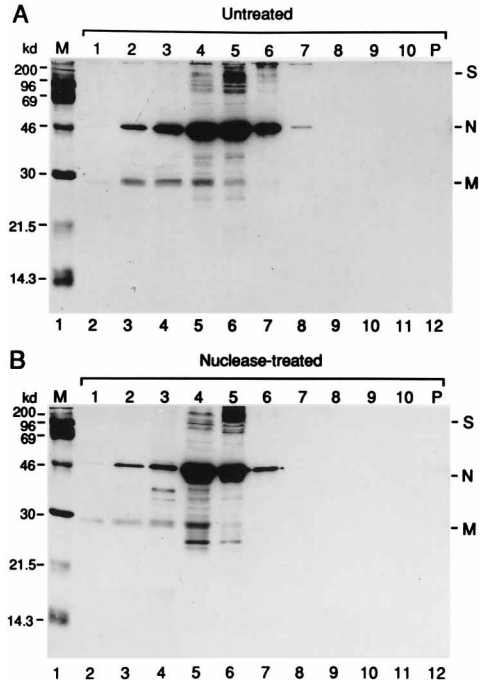

FIG. 5. TGEV-specific proteins in CsCl gradient fractions. Proteins recovered from the gradient shown in Fig. 3 were subjected to Western blot analysis. Porcine hyperimmune serum preadsorbed to uninfected cells was used. (A) Postnuclear fraction sedimented directly. Lane 1, molecular weight markers; lanes 2 to 11, gradient fractions 1 to 10; lane 12, gradient pellet. (B) Postnuclear fraction treated with micrococcal nuclease before sedimentation. Lanes are as defined for panel A.

omy of the replication complex known. Additionally, it is not known what barriers membranes might pose for the replication or transcription of exogenously added templates.

Here, with the use of CsCl gradients, we demonstrate the physical separation of RNA-containing membrane replication complexes of a coronavirus (11) on the basis of buoyant density. We learned that complexes prepared in this way are made up of at least two poorly defined but nevertheless distinct buoyant density groups. Curiously, two populations of RNA-dependent RNA polymerase-containing complexes were also resolved by isokinetic sedimentation in sucrose gradients in an earlier analysis of TGEV membrane-associated polymerase (11), but the relationship between these and the complexes identified here has not yet been determined. Although it cannot be expected that the physical character of the two sets of complexes in the separate experiments would necessarily be the same, since the high salt in the CsCl gradient might have removed adherent surface proteins or nucleic acids, or the intracomplex cation content might have been altered by a transmembrane exchange with Cs^+ (28), it is possible that the different methods of separation resolve the same two populations of structures. Interestingly, the existence of two populations of membrane-associated replication complexes is also consistent with the heterogeneous character of membranous vesicles observed by electron microscopy in coronavirus-infected cells (10, 12, 34). Vesicles which are the probable sites of RNA synthesis, based on intravesicular immunostaining with antipolymerase antibodies (3) and by analogy with the RNA-dependent RNA polymerase-containing structures in cells infected with picornavirus (4) and alphavirus (13), were shown to be heterogeneous with regard to both electron density and size (12).

Thus, it is tempting to speculate that the two populations of membranous complexes reflect structures having specialized function in RNA replication or transcription. Considering the data together, we envision that the denser complex might function primarily in the abundant synthesis of mRNAs and that the lighter complex might function in the synthesis of more or less equal amounts of minus and plus strands. Translation in (or near) either complex might happen only to the extent that it fulfills a possible *cis*-acting requirement for RNA replication (8). Such a system might allow for an uncoupling between the processes of translation and minus-strand RNA synthesis that would otherwise be competing for the same plus-strand template.

In addition to results showing minus-strand RNA species associating almost exclusively with membrane-protected structures, a most notable observation was that the genomic and subgenomic minus-strand RNAs in all cases were found to copartition among the buoyant subpopulations. This finding along with earlier data showing the template involvement of subgenomic minus strands (16, 29, 31, 33) supports the notion that the minus-strand species of all sizes function as templates for plus-strand RNA synthesis. Our data show, furthermore, that CsCl gradients might be useful for obtaining preparations of coronavirus membrane-associated replication complexes for the mechanistic analysis of replication and transcription. Successful recovery of functional RNA-dependent RNA polymerase-containing RNP complexes of negative-strand RNA viruses from CsCl gradients (23, 24, 26) suggests that CsCl is not necessarily intrinsically toxic to viral RNA polymerase and that active coronavirus replication complexes may be recoverable from CsCl gradients. Synthetic templates of known ability to replicate and transcribe in vivo, such as the genomes of coronavirus defective interfering RNAs, would appear to be molecules of choice for these studies.

ACKNOWLEDGMENTS

We thank David Hacker for helpful discussion of the data.

This work was supported primarily by Public Health Service grant AI 14367 from the National Institutes of Health and in part by funds from the University of Tennessee College of Veterinary Medicine Center of Excellence Program for Livestock Diseases and Human Health.

REFERENCES

1. **Barton, D. J., and J. B. Flanegan.** 1993. Coupled translation and replication of poliovirus RNA in vitro: synthesis of functional 3D polymerase and infectious virus. J. Virol. **67:**822–831.
2. **Barton, D. J., S. G. Sawicki, and D. L. Sawicki.** 1991. Solubilization and immunoprecipitation of alphavirus replication complexes. J. Virol. **65:**1496–1506.
3. **Bi, W., P. J. Bonilla, K. V. Holmes, S. R. Weiss, and J. L. Leibowitz.** 1995. Intracellular localization of polypeptides encoded in mouse hepatitis virus open reading frame 1A. Adv. Exp. Med. Biol. **380:**251–258.
4. **Bienz, K., D. Egger, T. Pfister, and M. Troxler.** 1992. Structural and functional characterization of the poliovirus replication complex. J. Virol. **66:** 2740–2747.
5. **Brayton, P. R., S. A. Stohlman, and M. M. C. Lai.** 1984. Further characterization of mouse hepatitis virus RNA-dependent RNA polymerase. Virology **133:**197–201.
6. **Brian, D. A., D. E. Dennis, and J. S. Guy.** 1980. Genome of porcine transmissible gastroenteritis virus. J. Virol. **34:**410–415.
7. **Brian, D. A., R.-Y. Chang, P. B. Sethna, and M. A. Hofmann.** 1994. Role of subgenomic minus-strand RNA in coronavirus replication. Arch. Virol. Suppl. **9:**173–180.
8. **Chang, R.-Y., and D. A. Brian.** 1996. *cis* requirement for N-specific protein sequence in bovine coronavirus defective interfering RNA replication. J. Virol. **70:**2201–2207.
9. **Chang, R.-Y., R. Krishnan, and D. A. Brian.** 1996. The UCUAAAC promoter motif is not required for high-frequency leader recombination in bovine coronavirus defective interfering RNA. J. Virol. **70:**2720–2729.
10. **David-Ferriera, J. F., and R. A. Manaker.** 1965. An electron microscope

study of the development of a mouse hepatitis virus in tissue culture cells. J. Cell Biol. **24:**57–78.
11. **Dennis, D. E., and D. A. Brian.** 1982. RNA-dependent RNA polymerase activity in coronavirus-infected cells. J. Virol. **42:**153–164.
12. **Dubois-Dakcq, M., K. V. Holmes, and B. Rentier.** 1984. Assembly of coronaviruses, p. 100–117. *In* D. W. Kingsbury (ed.), Assembly of enveloped RNA viruses. Springer-Verlag, New York, N.Y.
13. **Froshauer, S., J. Kartenbeck, and A. Helenius.** 1988. Alphavirus RNA replicase is located on the cytoplasmic surface of endosomes and lysosomes. J. Cell Biol. **107:**2075–2086.
14. **Hiscox, J. A., K. L. Mawditt, D. Cavanagh, and P. Britton.** 1995. Investigation of the control of coronavirus subgenomic mRNA transcription by using T7-generated negative-sense RNA transcripts. J. Virol. **69:**6219–6227.
15. **Hofmann, M. A., and D. A. Brian.** 1991. The 5-prime end of coronavirus minus-strand RNAs contains a short poly(U) tract. J. Virol. **65:**6331–6333.
16. **Hofmann, M. A., P. B. Sethna, and D. A. Brian.** 1990. Bovine coronavirus mRNA replication continues throughout persistent infection in cell culture. J. Virol. **64:**4108–4114.
17. **Kapke, P. A., and D. A. Brian.** 1986. Sequence analysis of the porcine transmissible gastroenteritis coronavirus nucleocapsid protein gene. Virology **151:**41–49.
18. **Kapke, P. A., F. Y. T. Tung, B. G. Hogue, D. A. Brian, R. D. Woods, and R. Wesley.** 1988. The amino-terminal signal peptide on the porcine transmissible gastroenteritis coronavirus matrix protein is not an absolute requirement for membrane translocation and glycosylation. Virology **165:**367–376.
19. **Lai, M. M. C.** 1990. Coronavirus: organization, replication, and expression of genome. Annu. Rev. Microbiol. **44:**303–333.
20. **Mahy, B. W. J., S. Siddell, H. Wege, and V. ter Meulen.** 1983. RNA-dependent RNA polymerase activity in murine coronavirus-infected cells. J. Gen. Virol. **64:**103–111.
21. **Miller, W. A., and T. C. Hall.** 1983. Use of micrococcal nuclease in the purification of highly template dependent RNA-dependent RNA polymerase from brome mosaic virus-infected barley. Virology **125:**236–241.
21a. **Moreau, K., and D. Brian.** Unpublished data.
22. **Morimoto, T., M. Arpin, and S. Gaetani.** 1983. Use of proteases for the study of membrane insertion. Methods Enzymol. **96:**121–150.
23. **Naito S., and A. Ishihama.** 1976. Function and structure of RNA polymerase of vesicular stomatitis virus. J. Biol. Chem. **251:**4307–4314.
24. **Parvin, J. D., P. Palese, A. Honda, A. Ishihama, and M. Krystal.** 1989. Promoter analysis of influenza virus RNA polymerase. J. Virol. **63:**5142–5152.
25. **Penman, S., H. Greenberg, and M. Willems.** 1968. Preparation of polyribosomes from cells grown in tissue culture, p. 49–58. *In* K. Habel and N. P. Salzman (ed.), Fundamental techniques in virology. Academic Press, New York, N.Y.
26. **Pons, M. W., I. T. Schulze, G. K. Hirst, and R. Hauser.** 1969. Isolation and characterization of the ribonucleoprotein of influenza virus. Virology **39:**250–259.
27. **Raju, R., L. Raju, D. Hacker, D. Garcin, R. Compans, and D. Kolakofsky.** 1990. Nontemplated bases at the 5′ ends of Tacaribe virus mRNAs. Virology **174:**53–59.
28. **Sachs, A. B., B. Lenchitz, R. L. Noble, and G. P. Hess.** 1982. A convenient large-scale method for the isolation of membrane vesicles permeable to a specific inorganic ion: isolation and characterization of functional acetylcholine receptor-containing vesicles from the electric organ of Electrophorus electricus. Anal. Biochem. **124:**185–190.
29. **Sawicki, S. G., and D. L. Sawicki.** 1990. Coronavirus transcription: subgenomic mouse hepatitis virus replicative intermediates function in RNA synthesis. J. Virol. **64:**1050–1056.
30. **Sawicki, S. G., and D. L. Sawicki.** 1995. Coronavirus use discontinuous extension for synthesis of subgenome-length negative strands. Adv. Exp. Med. Biol. **380:**499–506.
31. **Schaad, M. C., and R. S. Baric.** 1994. Genetics of mouse hepatitis virus transcription: evidence that subgenomic negative strands are functional templates. J. Virol. **68:**8169–8179.
32. **Sethna, P. B., and M. A. Hofmann, and D. A. Brian.** 1991. Minus-strand copies of replicating coronavirus mRNAs contain antileaders. J. Virol. **65:**320–325.
33. **Sethna, P. B., S.-L. Hung, and D. A. Brian.** 1989. Coronavirus subgenomic minus-strand RNA and the potential for mRNA replicons. Proc. Natl. Acad. Sci. USA **86:**5626–5630.
34. **Sturman, L. S., and K. V. Holmes.** 1983. The molecular biology of coronaviruses. Adv. Virus Res. **28:**25–112.
35. **Sturman, L. S., K. V. Holmes, and J. Behnke.** 1980. Isolation of coronavirus envelope glycoproteins and interaction with the viral nucleocapsid. J. Virol. **33:**449–462.
36. **Tooze, J., S. Tooze, and G. Warren.** 1984. Replication of coronavirus MHV-A59 in sac$^-$ cells: determination of the first site of budding of progeny virions. Eur. J. Cell Biol. **33:**281–293.
37. **Tung, F. Y. T., S. Abraham, M. Sethna, S.-L. Hung, P. B. Sethna, B. G. Hogue, and D. A. Brian.** 1992. The 9.1 kilodalton protein hydrophobic protein encoded at the 3′ end of the porcine transmissible gastroenteritis coronavirus genome is membrane associated. Virology **186:**676–683.
38. **Wu, S.-X., P. Ahlquist, and P. Kaesberg.** 1992. Active complete in vitro replication of nodavirus RNA requires glycerophospholipid. Proc. Natl. Acad. Sci. USA **89:**11136–11140.
39. **Wu, S.-X., and P. Kaesberg.** 1991. Synthesis of template-sense, single-strand flockhouse virus RNA in a cell-free replication system. Virology **183:**392–396.